Charles University, Faculty of Mathematics and Physics

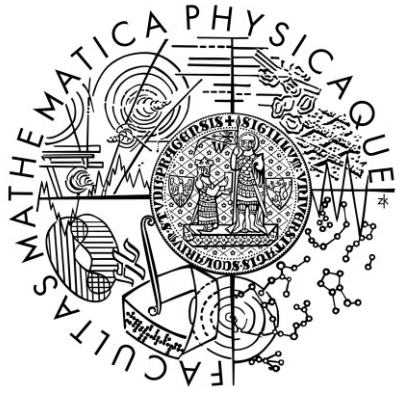

Combined STM/AFM on Oxide Surfaces: From TiO_2 to Ternary Compounds

Habilitation Thesis

Martin Setvín

Prague, 2018

Table of Contents

Author's note:

A shorter version of this habilitation thesis has already been successfully defended at the TU Wien (Austria) in 2018, and Martin Setvin has been awarded by the academic title "Privatdozent' for it. I am submitting an extended version of the same work to Charles University in Prague (Faculty of Mathematics and Physics) to verify that my research work meets the criteria requested for an equivalent position (Docent). Unfortunately, academic institutes in Czech Republic generally do not accept habilitations from other countries, therefore repeating the habilitation procedure is a necessary step to be able to apply for an academic position in my home country.

The Thesis previously defended at TU Wien is entitled:
M. Setvin, "*The surface Science of TiO_2: Focus on Anatase*", Habilitation Thesis, TU Wien, Vienna, Austria, 2017

Introduction and Overview

This habilitation thesis summarizes the research from my postdoc stay at the Vienna University of Technology, plus selected results from my continued Assistant Professor position at the same institute. My 3.5-year postdoc in Vienna was mostly focused on the surface science of titanium dioxide. Titania is a versatile material, which has been staying at the forefront of materials research for more than 40 years, since the discovery of the photocatalytic water splitting by Fujishima and Honda [1]. Currently it is the best understood metal oxide and it is often considered a prototype for other binary metal oxides.

In the last decade, the scientific interest in titania was mostly pushed by the need to generate and store energy from renewable sources. TiO_2 was mainly investigated for the purposes of photocatalytic fuel generation [2] and photovoltaics (dye-sensitized solar cells) [3,4]. There is also an increasing interest in its electronic properties as a transparent conducting oxide (TCO) [5], its memristive behavior [6-8], or in gas sensing applications [9]. It is also a good cathode material for lithium storage in Li-ion batteries [10,11]. The popularity of TiO_2 stems from its low cost, high stability in ambient conditions, and high resistance against photocorrosion. Further, TiO_2 powders are already produced in huge quantities for trivial applications like pigments for wall paints and clothes, UV-filtration in sunscreens, and many others.

There are several polymorphs of TiO_2 [12], but two of them play a prominent role in applications – rutile and anatase. Rutile is the most stable crystal structure and huge efforts have been invested into its fundamental research. On the other hand, the metastable anatase phase is more effective or appropriate for a vast majority of the aforementioned applications. There is significantly less fundamental knowledge about anatase surfaces, mostly due to experimental complications related to its metastable character (for illustration, available single-crystal samples are shown in Figure 1). My research was strongly oriented in direction of the anatase polymorph, and characterizing its differences from the rutile phase.

Section 1, focused on TiO_2, is structured into four subsections. The first subsection (publications A1-A7) centers around the electronic properties and defect chemistry of the anatase TiO_2 (101) surface, in comparison with the prototypical rutile (110). The second subsection (publications A8-A12) discusses the role of

excess electrons in the surface chemistry of the anatase and rutile. The third subsection (A13-A14) deals with mechanistic details of photoinduced reactions, where methanol photodecomposition was used as a prototypical reaction. The last publication (A15) describes details of the used materials and surface preparation, which are key for investigating the metastable anatase polymorph.

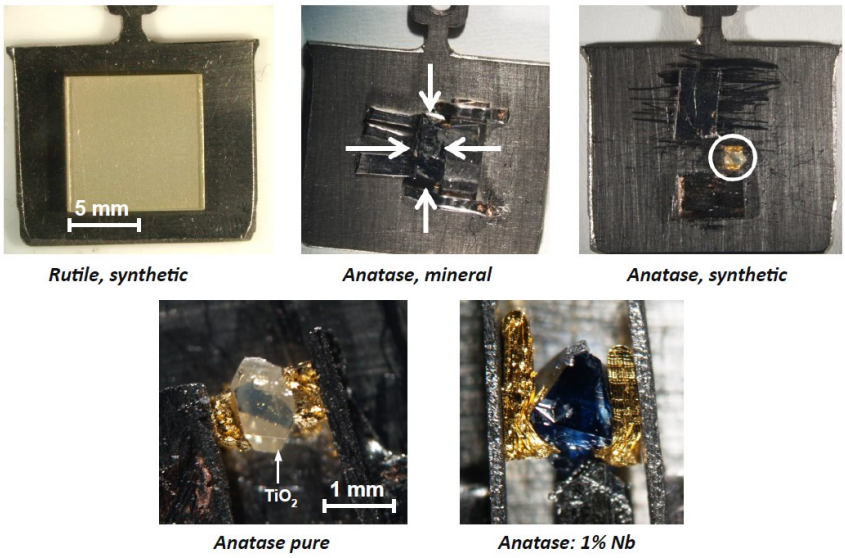

Figure 1: TiO_2 single crystals used for research. *Rutile is commercially available in the form of large synthetic single crystals with negligible impurity levels. Mineral anatase samples are several mm in size, but typical impurity levels are on order of percent. The largest synthetic anatase samples are typically only ~1 mm in size.*

While my research of TiO_2 was based on the Scanning Tunneling Microscopy (STM) as the main analytical tool, my second task in Vienna was 'promoting' the noncontact Atomic Force Microscopy (nc-AFM) in the field of oxide surface science. AFM is widely used in ambient conditions in many modifications, but one particular setup has recently emerged as a very powerful analytical tool – the noncontact AFM combined with STM. In the past decade, this combination has demonstrated for example an enhanced chemical resolution [13], manipulation of single electrons [14], or submolecular resolution of organic molecules [15]. The field of nc-AFM is currently strongly biased towards the organic molecules, while other research directions are overlooked and still offer many exciting opportunities. The last Section of this Thesis will demonstrate selected results, which outline various options offered by the nc-AFM technique in the research of complex materials (publications A16-A18).

Section 1: TiO_2 Anatase and Rutile

Electronic Properties and Defect Chemistry

Charge carriers in the bulk crystal lattice

Rutile and anatase, the two main polymorphs of TiO_2, have the identical chemical formula, but there is a significant difference in their performance in applications. For example, anatase is usually assumed to be more active in photocatalysis compared to rutile. Further, anatase can be used as a transparent conducting material in LCD displays or LED diodes [16], while the same property cannot be achieved with rutile. Also, dye-sensitized solar cells exclusively use the anatase phase, while rutile shows poor performance.

We have found several key differences between the two polymorphs. The first difference lies in the interaction of charge carriers with a perfect bulk material; specifically there is a different mechanism for polaron formation (publication A1). When an electron is donated to a bulk crystal lattice of rutile, it localizes at a single Ti atom and forms so-called small polaron [17,18]. The polaron can hop to neighboring lattice sites, but such motion requires thermal activation. The situation is different in anatase: An electron donated to a perfect bulk lattice keeps a delocalized (band-like) configuration, resulting in metal-like electrical conductivity. In anatase, electrons can only become localized at lattice defects (such as, e.g., oxygen vacancies) or steps (publication A2).

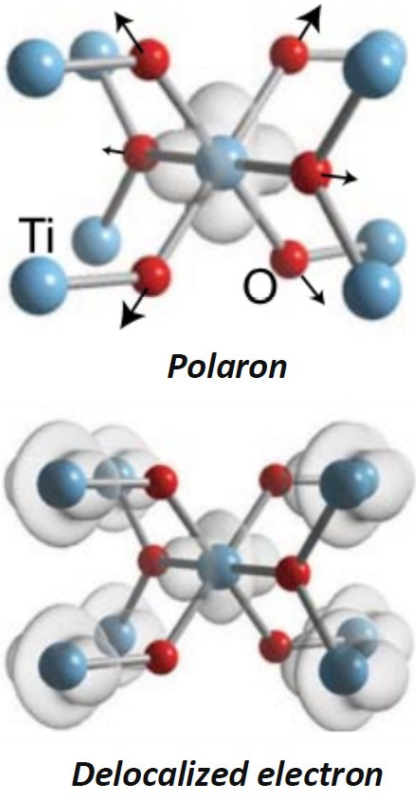

Figure 2: *Excess charge density of a polaron and a delocalized electron in bulk rutile. Arrows denote lattice distortions responsible for the electron self-trapping. Adopted from ref. [18]*

The mechanism of polaron formation immediately explains the difference in electrical conductivity of rutile and anatase. Niobium-doped anatase is transparent [5] and shows a metal-type conductivity, even when cooled to cryogenic temperatures. Rutile with comparable doping is black, the electrical resistance is three

orders of magnitude higher, and its electrical resistivity has a semiconductor-like temperature dependence [16].

Notably, theoretical works predict that photoexcited holes have the opposite behavior in the two materials [19]: Small hole-polarons should be formed in anatase, while their delocalized character should be preserved in rutile. Unlike for electrons, there is very little direct experimental evidence for the hole-polaron formation/absence in anatase and rutile.

Oxygen vacancies

Another difference between rutile and anatase lies in the behavior of oxygen vacancies (V_Os). The rutile (110) is considered as a prototype oxide surface, and after a decade of research it was concluded that the surface oxygen vacancies play a key role in its surface chemistry [20]. The concentration of surface V_Os depends on the reduction state of the sample and varies from a few percent of surface lattice sites (for transparent crystals) up to ~17% for strongly reduced black crystals. The V_Os affect the materials surface chemistry in two ways: First, they represent reactive sites, which directly enter chemical reactions. Second, they donate excess electrons to the material, which can be transferred to adsorbed species and thus alter their chemical reactivity.

Surprisingly, the surface V_Os are completely absent on the anatase (101) surface [21]. DFT calculations predicted that these defects are more stable in the subsurface positions, which has been proven experimentally later [22]. The surface oxygen vacancies were created artificially be bombarding the surface with high-energy electrons, and it was demonstrated that these defects start to migrate to subsurface sites at temperatures as low as 200 K.

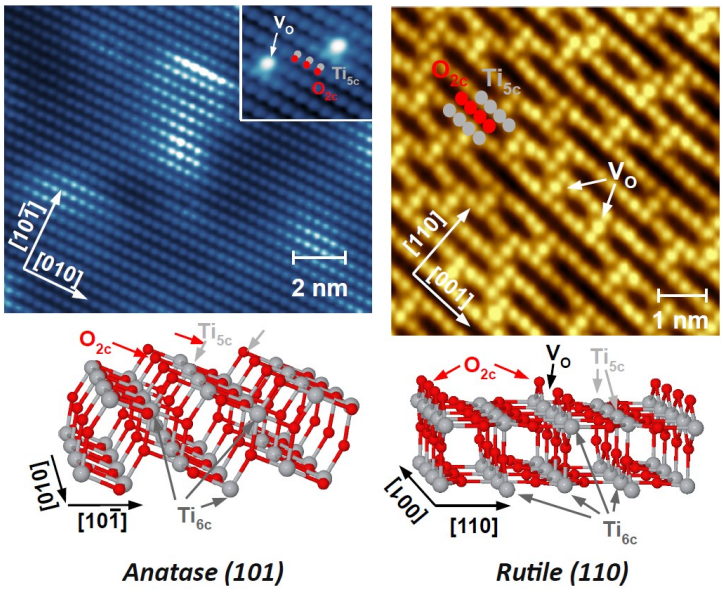

Figure 3: *Empty-states STM images of the anatase (101) and rutile (110) surfaces prepared under UHV conditions. The inset in the anatase image shows artificially-created oxygen vacancies. The respective surface structures are shown below.*

These findings brought a key question about the role of subsurface defects in the anatase surface chemistry. I have performed various experiments aiming to address this issue. First, I have tried to use simple probe molecules such as CO (publication A3). Previously-published theoretical predictions that CO adsorption above a subsurface Vo should result in enhanced electron back-donation into its pi-antibonding states [23]. This should be reflected in a significantly increased adsorption energy and weakening its C=O bonding, which should be measurable by infrared absorption spectroscopy. Such effect has been previously successfully demonstrated on the rutile (110) surface [24], however, our results on the anatase (101) surface clearly excluded this scenario (publication A3). This was a strong evidence against the presence of single oxygen vacancies residing in the near-surface region. Similar to our CO probe molecule, theoretical predictions have been made also for adsorption of H_2O above subsurface V_Os [25]. Such predictions also turned out to be inconsistent with the experimentally observed behavior [26].

Seeking a deeper understanding of the V_O behavior in anatase, I have performed further experimental work described in publication A4. Here the V_Os were artificially prepared by electron bombardment of the sample, and I succeeded in tracking their migration at temperatures between 200 and 350 K. It turned out that the vacancies first migrate subsurface, and then start forming clusters. It is possible to use the electric field of the STM tip to break up these clusters, and move the vacancies back to the surface (see Figure 4). This experiment proved that the V_Os tend to cluster in the material, and also allowed counting the number of V_Os incorporated in different types of clusters. These subsurface clusters disappear after annealing to temperatures above ~400^{O}C. It is still not completely clear what happens to the vacancies, but likely they agglomerate in extended defects such as glide planes.

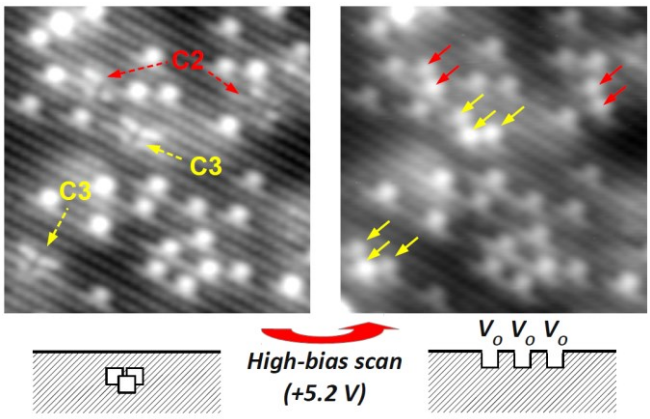

Figure 4: *Clusters of oxygen vacancies can be decomposed into characteristic Vo groupings by applying high bias.*

These experimental results prove that the oxygen vacancies do not play any direct role in the surface chemistry of the anatase (101). However, the reduced material still possesses excess electrons, which can be transferred to adsorbed species. It turned out that a suitable model for theoretical calculations of a reduced

anatase (101) surface can be obtained by incorporating hydrogen atoms in the slab or Niobium dopants in the subsurface region; both act as electron donors and their effect on the surface chemistry discussed below.

The defect chemistry of rutile and anatase is comprehensively summarized in a review paper A5. Also, a comparison with defect chemistry of other binary metal oxides (Fe_3O_4 and In_2O_3) is provided.

Influence of polarons on the materials structure

In publications A6 and A7 we have investigated the relation between the concentration of excess electrons and the surface geometric structure. It turns out that the polaron formation influences the surface topography: Each polaron occupies a certain space in the crystal lattice, and this condition plays a role already when the surface is being prepared by high-temperature annealing [27]. Publications A6-A7 were performed exclusively on the rutile (110) surface, because the electron polarons do not form for anatase (as explained above).

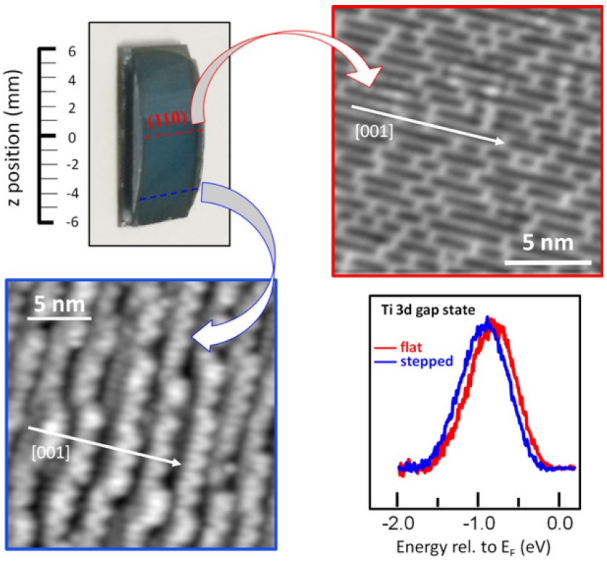

Figure 5: A rutile single crystal curved around the (110) plane. *The central regions show flat terraces, while the step density increases smoothly when moving to the sides. Photoemission shows only minor differences in the electronic structure of different regions.*

We have also made the first observations on the step edges of the rutile (110) surface, see publication A6. Here we used a special crystal, which was cut and polished into a slightly cylindrical shape (Figure 5). In this case, imaging different regions of the sample allowed studying a surface with varying step concentration. The step geometry and the distribution of terrace sizes turned out to dramatically depend on the reduction state of the crystal (*i.e.,* concentration of V_Os and excess electrons).

Interestingly, the steps on rutile have rather limited influence on the surface electronic structure and on the surface chemistry. This situation is very different from the observations made on the anatase (publication A2), and we attribute this to the fact that rutile can form small polarons at any lattice site, thus the role of a step is less important than on the anatase, where the electron trapping occurs exclusively at the steps.

The relation between the polarons and the surface morphology is investigated in detail in publication A7. This work was motivated by two experimental observations, which have been known for a long time, but had remained unexplained so far. First, the V_O concentration on the rutile has a magic threshold of 16.7%. When this limit is exceeded, the surface starts forming a different phase organized in a (1x2) reconstruction. Second, occupied-states STM images of highly reduced rutile surfaces show that the polarons are arranged in a periodic (3×1) pattern, even though their source – oxygen vacancies – do not have this periodicity. Phrased colloquially [27], a polaron can be understood as a brick, which has a size of three lattice sites. Squeezing a polaron into a smaller volume is energetically very unfavorable, instead the material prefers formation of a different crystal phase.

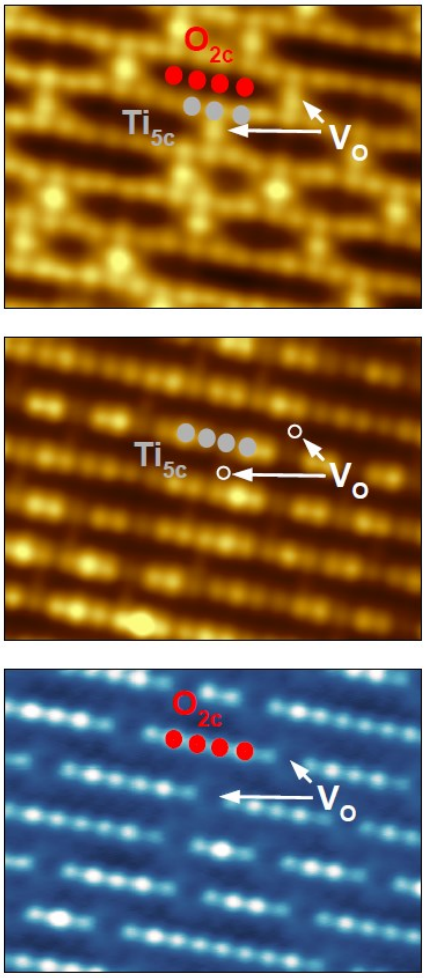

Figure 6: Polaron ordering on the rutile (110) surface. *The filled-states STM image (middle) shows that the density of excess electrons exhibits ordering with a (3x1) periodicity. The empty-states STM image (top) and the constant-height AFM image (bottom) of the same region show the V_O distribution.*

Role of Excess Electrons in Surface Chemistry

The key to photocatalysis lies in the electron transfer between the substrate and an adsorbed molecule. Electron transfer into the adsorbed molecule represents chemical reduction, while hole transfer (electron transfer from the molecule) represents the chemical oxidation of an adsorbed molecule. Oxide samples prepared in ultrahigh vacuum are typically reduced, thus they possess excess electrons, which are available for initiating reduction reactions, even without any photo-excitation.

This section uses O_2 as a prototypical electron-accepting molecule, and combined STM/AFM is used to directly image chemical reactions enabled by this charge transition. O_2 is a molecule with unique properties: It is completely inert in its neutral form, which stems from the fact that its lowest-energy state has a spin triplet configuration. In catalysis, the molecule is activated by transferring an electron to the molecule. Such activated molecules (superoxo or peroxo with one or two extra electrons, respectively), can readily enter chemical reactions.

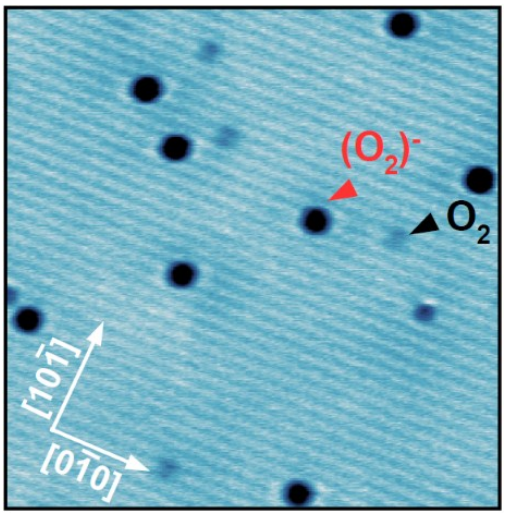

Figure 7: *A constant-height AFM image of O_2 adsorbed on the anatase (101) surface. The chemical difference between neutral O_2 molecules and negatively charged radicals is clearly visible.*

Publication A8 is based on STM results combined with DFT calculations and explains the interaction of O_2 with the anatase (101) substrate. It focuses on several different adsorption configurations and on the role of oxygen vacancies and Nb dopants in the process. Publication A9 focuses solely on the problem of transferring the first electron into the adsorbing molecule; here the unique abilities of noncontact AFM are used to image the neutral and negatively charged O_2 species (see Figure 7). At the same time, the independent STM function of this instrument can be used to manipulate at will the charge state of single molecules.

The chemical reactivity of such an activated $(O_2)^-$ molecule is described in detail in publication A10. These species can react with water, and this reaction (called oxygen reduction reaction) plays a prominent role in the chemistry of O_2, because water is abundant in ambient conditions. This work describes in detail how this reaction cascade proceeds, and discusses the energy balance of single reaction

steps, which depend on the number of available electrons donated by the anatase substrate into the reaction.

The role of excess electrons is most pronounced when they are transferred to the adsorbed species, like in the case of O_2. However, even excess charge present in the substrate can significantly influence the adsorbate. This is demonstrated in publication A11 on the example of CO adsorption on the rutile TiO_2 (110) surface. There the excess electrons form polarons, and the CO molecules can couple to these polarons, which in turn influences their adsorption energy, the strength of the C=O bond, and the reactivity.

The last publication (A12) in this section is focused mainly on the issue of STM imaging of such adsorbed species and their chemical reactions. Many of these reaction intermediates have a very similar appearance in STM images, and this work proposes a technique for identifying these species based on chemical changes induced when higher bias is applied on the STM tip.

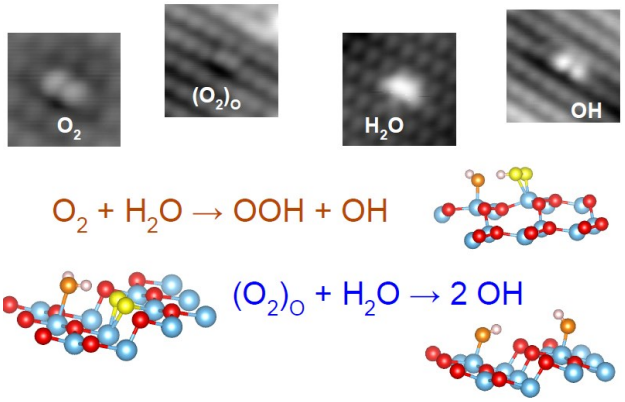

Figure 7: *Selected reaction steps from the oxygen reduction reaction on the anatase (101) surface.*

Mechanistic Insights into the Photocatalysis of Methanol

This part of my research aimed to obtain a detailed understanding of photocatalytic reactions occurring at the anatase surface. Publication A13 explains with unprecedented detail photoinduced reactions of methanol. Publication A14 resolves the adsorption of formaldehyde. The latter work has been performed mainly because formaldehyde is the main reaction product of methanol photodecomposition, thus a detailed understanding of its adsorption was necessary for tracking methanol photocatalysis.

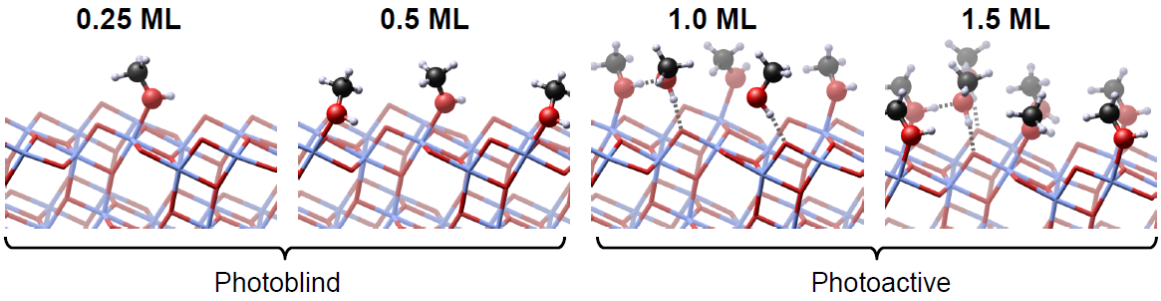

Figure 9: Coverage-dependent adsorption configurations of methanol. *Methanol is photoblind at low coverages, while it becomes photoactive above 0.5 monolayer (ML). The dashed lines mark hydrogen bonds.*

Methanol was selected as a prototypical molecule, which represents a large class of organic molecules binding to oxide surfaces in a monodentate configuration. Methanol is often used as a hole scavenger in applied photocatalysis, *i.e.*, it accepts photoexcited holes from TiO_2 powders. This is often used, for example, to suppress electron-hole recombination rates. Surprisingly, single methanol molecules turned out to be completely photo-blind on the anatase (101) surface, even after large doses of UV irradiation. It turned out that the molecule requires activation via a partial dissociation into a methoxy species (i.e., the removal of a hydrogen atom from its OH group). This was obtained in two different ways: First, by reaction with $(O_2)^-$ radicals, which readily accept hydrogen atoms from organic molecules. The second activation mechanism is rather surprising – it opens up at higher methanol coverages, and it stems from the formation of a hydrogen-bonded network within the layer of molecules. Notably, a similar work has been performed on the rutile (110) surface at the same time [28], showing exactly the opposite trend: There the photoactivity *decreased* with the coverage. This points to a significant role of the hydrogen-bonded network in photocatalysis and, notably, the role of geometric

arrangement of the substrate atoms, which dictates the arrangement of the H-bonding network.

Anatase Surfaces Suitable for Fundamental Studies

The last publication in this section (A15) provides a detailed characterization of the materials used and the experimental procedures that result in high-quality oxide surfaces suitable for such fundamental research. This publication focuses on bulk anatase single crystals. Notably, another experimental approach is based on growing anatase thin films; this type of samples are usually used for the (001) surface of anatase, where a reliable growth recipe is known [29].

Section 2: Noncontact AFM on Complex Oxides

Scanning tunneling microscopy (STM) is nowadays a conventional tool for investigating materials structure, electronic properties, and chemical processes occurring at surfaces. The past decade has brought a revolution in a related technique – noncontact atomic force microscopy (nc-AFM) [30]. After solving the initial difficulties with obtaining atomic resolution [31], AFM has been adapted for submolecular resolution of organic molecules [15], achieving superior chemical resolution [13], and controlling the charge state of single atoms and molecules [14].

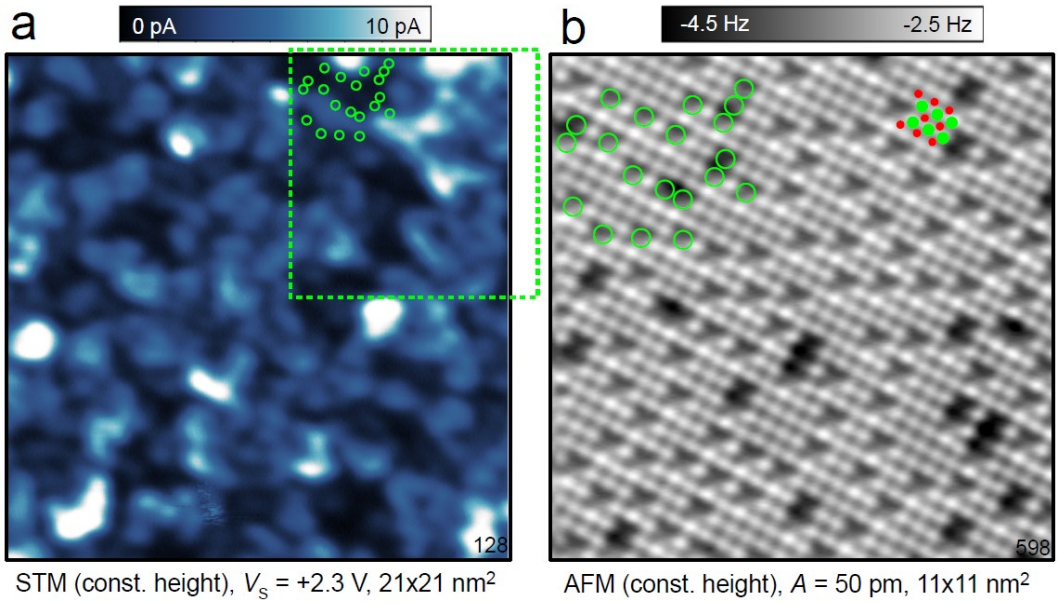

Figure 10: Bulk-terminated $SrTiO_3$ (001) surface. *a) STM image of a cleaved SrTiO3 crystal, showing the SrO-terminated surface. b) AFM image of the region marked in panel (a) by the dashed square.*

While some of the AFM results have already been presented above, this section demonstrates more options how the technique pushes forward our understanding of complex surfaces. Publications A16 and A17 are related to oxides with the perovskite structure – $KTaO_3$ and $SrTiO_3$. While binary oxides can be nowadays considered as well-understood materials, relatively little is known about surfaces of ternary compounds. Especially perovskites turned out to be very challenging. Figure 10 illustrates the advantages of AFM on an example of a cleaved $SrTiO_3$ (001) surface (Publication A17). This specific surface has been attracting great attention for approximately 25 years, yet I am not aware of any successful atomically-resolved study. The problem stems from the fact that conventional STM imaging does not provide atomic resolution, because the surface electronic structure

does not contain any suitable surface state. As a consequence, STM images (Fig. 10a) only show band-bending induced by surface defects and thus contain very little useful information. On the other hand, AFM images (Fig. 10b) show clear atomic resolution, and allow characterization of surface defects. This is the missing piece of knowledge in the surface science of perovskites and I believe that AFM will help with solving many open questions in the field.

Publication A18 shows the last example how AFM helps with understanding the surface chemistry. This work is focused on water adsorption on the magnetite Fe_3O_4 (001) surface. Our group in Vienna has been working on the system of magnetite + water already for 10 years. The main challenge lies in the high-coverage regime (first monolayer), where water forms hydrogen-bonded networks and partially dissociates. In general, hydrogen-bonded networks are difficult to image by STM, because the tunneling electrons easily switches hydrogen bonds [32]. As a result, STM only shows fuzzy images of the surface. AFM allows working without any tunneling current, thus resolving systems, where STM was prone to provide any useful information.

References

[1] A. Fujishima and K. Honda, Nature **37**, 238 (1972).

[2] Y. Ma, X. Wang, Y. Jia, X. Chen, H. Han, and C. Li, Chem. Rev. **114**, 9987−10043 (2014).

[3] B. O'Regan and M. Grätzel, Nature **353**, 737 (1991).

[4] M. Grätzel, Nature **414**, 338 (2001).

[5] Y. Furubayashi, T. Hitosugi, Y. Yamamoto, K. Inaba, G. Kinoda, Y. Hirose, T. Shimada, and T. Hasegewa, Appl. Phys. Lett. **86**, 252101 (2005).

[6] J. J. Yang, D. B. Strukov, and D. R. Stewart, Nature Nanotech. **8**, 13 (2013).

[7] K. Szot, M. Rogala, W. Speier, Z. Klusek, A. Besmehn, and R. Waser, Nanotechnology **22**, 1 (2011).

[8] K. Szot, G. Bihlmayer, and W. Speier, in *Solid State Physics* (Elsevier, Amsterdam, 2014), pp. 353.

[9] J. Bai and B. Zhou, Chem. Rev. **114**, 10131−10176 (2014).

[10] L. Kavan, M. Grätzel, S. E. Gilbert, C. Klemenz, and H. J. Scheel, J. Am. Chem. Soc. **118**, 6716 (1996).

[11] T.-F. Yi, S.-Y. Yang, and Y. Xie, J. Mat. Chem. A **3**, 5750 (2015).

[12] H. Zhang and J. F. Banfield, Chem. Rev. **114**, 9613−9644 (2014).

[13] Y. Sugimoto, P. Pou, M. Abe, P. Jelinek, R. Perez, S. Morita, and O. Custance, Nature **446**, 64 (2007).

[14] L. Gross, F. Mohn, P. Liljeroth, J. Repp, F. J. Giessibl, and G. Meyer, Science **324** (2009).

[15] L. Gross, F. Mohn, N. Moll, P. Liljeroth, and G. Meyer, Science **325**, 1110 (2009).

[16] S. X. Zhang, D. C. Kundaliya, W. Yu, S. Dhar, S. Y. Young, L. G. Salamanca-Riba, S. B. Ogale, R. D. Vispute, and T. Venkatesan, Journal Of Applied Physics **102**, 013701 (2007).

[17] I. G. Austin and N. F. Mott, Adv. Phys. **50**, 757 (2001).

[18] A. Janotti, C. Franchini, J. B. Varley, G. Kresse, and C. G. V. d. Valle, Phys. Stat. Sol. **7**, 199 (2013).

[19] P. Deak, B. Aradi, and T. Frauenheim, Phys. Rev. B **86**, 195206 (2012).

[20] U. Diebold, Surf. Sci. Rep. **48**, 53 (2003).

[21] Y. He, O. Dulub, H. Cheng, A. Selloni, and U. Diebold, Phys. Rev. Lett. **102**, 106105 (2009).

[22] P. Scheiber, M. Fidler, O. Dulub, M. Schmid, U. Diebold, W. Hou, U. Aschauer, and A. Selloni, Physical Review Letters **109**, 136103 (2012).
[23] P. G. Lustemberg and D. A. Scherlis, J. Chem. Phys. **138**, 124702 (2013).
[24] M. Xu, H. Noei, K. Fink, M. Muhler, Y. Wang, and C. Wöll, Angew. Chem. Intl. Ed. **51**, 4731 (2012).
[25] Y. Li and Y. Gao, Phys. Rev. Lett. **112**, 206101 (2014).
[26] Y. He, A. Tilocca, O. Dulub, A. Selloni, and U. Diebold, Nature Materials, 585 (2009).
[27] G. Pacchioni, Nat. Mater. Rev., doi:10.1038/natrevmats.2017.71 (2017).
[28] W. Yang, Z. Geng, Q. Guo, D. Dai, and X. Yang, J. Phys. Chem. C **121**, 17244 (2017).
[29] S. A. Chambers, C. M. Wang, S. Thevuthasan, T. Droubay, D. E. McCready, A. S. Lea, V. Shutthanandan, and C. F. Windisch, Thin Sol. Films **418**, 197 (2002).
[30] F. J. Giessibl, Rev. Mod. Phys. **75**, 949 (2003).
[31] F. J. Giessibl, Science **267**, 68 (1995).
[32] T. Kumagai, M. Kaizu, S. Hatta, H. Okuyama, T. Aruga, I. Hamada, and Y. Morikawa, Phys. Rev. Lett. **100**, 161101 (2008).

APPENDIX A: Core publications

(* corresponding author)

A1.* M. Setvin, C. Franchini, X. Hao, M. Schmid, A. Janotti, M. Kaltak, C. G. Van de Walle, G. Kresse, U. Diebold

Direct View at Excess Electrons in TiO_2 Rutile and Anatase

Phys. Rev. Lett. **113**, 086402 (2014)

Contribution of M. Setvin: Performed all experiments and data analysis, wrote the paper

A2.* M. Setvin, H. Hao, B. Daniel, J. Pavelec, Z. Novotny, G. S. Parkinson, M. Schmid, G. Kresse, C. Franchini, U. Diebold

Charge Trapping at Step Edges of TiO_2 Anatase (101)

Angew. Chem. Intl. Ed. **53**, 4714-4716 (2014)

Contribution of M. Setvin: Performed all experiments and data analysis, wrote the paper

A3.* M. Setvin, M. Buchholz, W. Hou, C. Zhang, B. Stoger, J. Hulva, T. Simschitz, X. Shi, J. Pavelec, G. S. Parkinson, M. Xu, Y. Wang, M. Schmid, Ch. Woll, A. Selloni, U. Diebold

A Multitechnique Study of CO adsorption on the TiO_2 Anatase (101) surface

J. Phys. Chem. C **119**, 21044-21052 (2015)

Contribution of M. Setvin: Performed STM experiments and data analysis, wrote the paper

A4.* M. Setvin, M. Schmid, U. Diebold

Aggregation and Electronically Induced Migration of Oxygen Vacancies in TiO_2 Anatase

Phys. Rev. B **91**, 195403 (2015)

Contribution of M. Setvin: Performed all experiments and data analysis, wrote the paper

A5. M. Setvin, M. Wagner, M. Schmid, G. S. Parkinson, U. Diebold

Surface Point Defects on Bulk Oxides: Atomically-Resolved Scanning Probe Microscopy

Chem. Soc. Rev. **46**, 1772-1784 (2017)

Contribution of M. Setvin: Wrote 40% of the paper.

A6. L. A. Miccio, M. Setvin, M. Muller, M. Abadia, I. Piquero, J. Lobo-Checa, F. Schiller, C. Rogero, M. Schmid, D. Sanchez-Portal, U. Diebold, J. E. Ortega

Interplay between Steps and Oxygen Vacancies on Curved TiO_2 (110)

Nanoletters **16**, 2017-2022 (2016)

Contribution of M. Setvin: Contributed to performing the STM experiments and to the paper writing

A7.* M. Reticcioli, M. Setvin, X. Hao, P. Flauger, G. Kresse, M. Schmid, U. Diebold, C. Franchini
Polaron-Driven Surface Reconstructions
Phys. Rev. X **7**, 031053 (2017)

Contribution of M. Setvin: Performed all STM and AFM experiments and contributed to writing the paper

A8. M. Setvin, U. Aschauer, P. Scheiber, Y.-F. Li, W. Hou, M. Schmid, A. Selloni, U. Diebold
Reaction of O_2 with Subsurface Oxygen Vacancies on TiO_2 anatase (101)
Science **341**, 988-991 (2013)

Contribution of M. Setvin: Performed all experiments, contributed to writing the paper

A9.* M. Setvin, J. Hulva, G. S. Parkinson, M. Schmid, U. Diebold
Electron Transfer Between Anatase TiO_2 and an O_2 molecule Directly Observed by Atomic Force Microscopy
Proc. Natl. Acad. Sci. **114**, E2556-E2562 (2017)

Contribution of M. Setvin: Performed all STM and AFM experiments, wrote the paper

A10.* M. Setvin, U. Aschauer, J. Hulva, T. Simschitz, B. Daniel, M. Schmid, A. Selloni, U. Diebold
Following the Reduction of Oxygen on TiO_2 Anatase (101) Step by Step
J. Am. Chem. Soc. **138**, 9565-9571 (2016)

Contribution of M. Setvin: Performed all STM experiments and data analysis, wrote the paper

A11.* M. Reticcioli, I. Sokolovic, M. Schmid, U. Diebold, M. Setvin, C. Franchini
Interplay between adsorbates and polarons: CO on Rutile TiO_2 (110)
Phys. Rev. Lett. **122**, 016805 (2019)

Contribution of M. Setvin: Designed the experimental work, contributed to analysis of the results and writing the paper

A12.* M. Setvin, B. Daniel, U. Aschauer, W. Hou, Y.-F. Li, M. Schmid, A. Selloni, U. Diebold
Identification of Adsorbed Molecules via STM Tip Manipulation: CO, H_2O, and O_2 on TiO_2 Anatase (101)
Phys. Chem. Chem. Phys. **16**, 21524-21530 (2014)

Contribution of M. Setvin: Performed all experiments and data analysis, wrote the paper

A13.* M. Setvin, X. Shi, J. Hulva, T. Simschitz, G. S. Parkinson, M. Schmid, C. Di Valentin, A. Selloni, U. Diebold

Methanol on Anatase TiO_2 (101): Mechanistic Insights into Photocatalysis

ACS Catalysis **7**, 7081-7091 (2017)

Contribution of M. Setvin: Performed part of the STM experiments and data analysis, wrote the paper

A14.* M. Setvin, J. Hulva, H. Wang, T. Simschitz, M. Schmid, G. S. Parkinson, C. Di Valentin, A. Selloni, U. Diebold

Formaldehyde Adsorption on the Anataase TiO_2 (101) Surface: Experimental and Theoretical Investigation

J. Phys. Chem. C **121**, 8914-8922 (2017)

Contribution of M. Setvin: Performed part of the STM/AFM experiments and data analysis, wrote the paper

A15.* M. Setvin, B. Daniel, V. Mansfeldova, L. Kavan, P. Scheiber, M. Fidler, M. Schmid, U. Diebold

Surface Preparation of TiO_2 Anatase (101): Pitfalls and how to avoid them

Surf. Sci. **626**, 61-67 (2014)

Contribution of M. Setvin: Performed all STM experiments, wrote the paper

A16.* M. Setvin, M. Reticcioli, F. Poelzleitner, J. Hulva, M. Schmid, L. A. Boatner, C. Franchini, U. Diebold

Polarity compensation mechanisms on the perovskite surface $KTaO_3$ (001)

Science **359**, 572-575 (2018)

Contribution of M. Setvin: Designed the experiments, measured part of the experimental data, wrote the paper

A17.* I. Sokolovic, M. Schmid, U. Diebold, M. Setvin

Incipient ferroelectricity: A route towards bulk-terminated $SrTiO_3$ (001)

Phys. Rev. Materials, accepted (2019)

ArXiv 1807.09379

Contribution of M. Setvin: Designed the research, contributed to the experiments and paper writing

A18.* M. Maier, J. Hulva, Z. Jakub, J. Pavelec, M. Setvin, R. Bliem, M. Schmid, U. Diebold, C. Franchini, G. S. Parkinson

Water Agglomerates on Fe_3O_4 (001)

Proc. Natl. Acad. Sci. **115**, E5642-E5650 (2018)

Contribution of M. Setvin: Designed the AFM experiments, contributed to writing the paper